# Aberrant Expression of the Tight Junction Molecules Claudin-1 and Zonula Occludens-1 Mediates Cell Growth and Invasion in Oral Squamous Cell Carcinoma

Hamzah Babkair[a,b],

Manabu Yamazaki[a] , Md. Shihab Uddin[a], Satoshi Maruyama[c], Tatsuya Abé[a,c], Ahmed Essa[a], Yoshimasa Sumita[a], Md. Shahidul Ahsan[a], Wael Swelam[b], Jun Cheng[a], Takashi Saku[a, c]

[a] Division of Oral Pathology, Niigata University Graduate School of Medical and Dental Sciences, Niigata, Japan

[b] Division of Oral Pathology, Department of Oral Basic and Clinical Sciences, College of Dentistry, Taibah University, Medina, Saudi Arabia

[c] Oral Pathology Section, Department of Surgical Pathology, Niigata University Hospital, Niigata, Japan

## Summary

We reported that altered cell contact mediated by E-cadherin is an initial event in the pathogenesis of oral epithelial malignancies. To assess other effects of cell adhesion, we examined the expression levels of tight junction (TJ) molecules in oral carcinoma in-situ (CIS) and squamous cell carcinoma (SCC). To identify changes in the expression of TJ molecules, we conducted an analysis of the immunohistochemical profiles of claudin-1 (CLDN-1) and zonula occludens-1 (ZO-1) in surgical specimens acquired from patients with oral SCC containing foci of epithelial dysplasia or from patients with CIS. We used immunofluorescence, western blotting, reverse transcriptase-polymerase chain reaction, and RNA interference (RNAi) to evaluate the functions of CLDN-1 and ZO-1 in cultured oral SCC cells. TJ molecules were not detected in normal oral epithelial tissues but were expressed in SCC/CIS cells. ZO-1 was localized within the nucleus of proliferating cells. When CLDN-1 expression was inhibited by transfecting cells with specific small interference RNAs, SCC cells dissociated, and their ability to proliferate and invade Matrigel was inhibited. In contrast, although RNAi-mediated inhibition of ZO-1 expression did not affect cell morphology, it inhibited cell proliferation and invasiveness. Our findings indicated that the detection of TJ molecules in the oral epithelia may serve as a marker for the malignant phenotype of cells in which CLDN-1 regulates proliferation and invasion.

Keywords: oral mucosa; squamous cell carcinoma; carcinoma in-situ; claudin-1; zonula occludens-1; tight junction; cell growth; invasion

## 1. Introduction

Dysregulation of cell adhesion, including cell-cell and cell-extracellular matrix (ECM) contacts, is a characteristic feature of multistep carcinogenesis and is associated with tumor progression [1]. Loss of cell-cell contact promotes the dissociation of cancer cells from their sites of origin, leading to invasion of adjacent tissues and metastasis [2]. Moreover, altered cell adhesion modulates gene activity via cell-cell junction-to-nuclear pathways such as β-catenin signaling [3]. We reported that loss of E-cadherin expression and nuclear translocation of β-catenin is associated with cell proliferation in oral epithelial dysplasia and carcinoma in-situ (CIS) [4]. Recently, tight junction (TJ) proteins have attracted attention as important modulators of cancer cell functions [5, 6].

TJ, which serves as a cell adhesion device for glandular epithelial cells or vascular endothelial cells that form luminal spaces, maintains cell polarity (fence function) and regulates fluid flow (barrier function) [7]. Further, TJs are present in stratified squamous epithelia such as the epidermis [8]. TJs contribute to the activities of signaling pathways that mediate cell proliferation and differentiation under pathophysiological conditions such as mammary gland development and breast cancer [6, 9].

The primary constituents of TJs are members of the claudin (CLDN) family, which comprises at least 27 members [6]. For example, the function of CLDN-1 is the subject of intensive investigations. In epidermal keratinocytes, CLDN-1 deficiency causes abnormal keratinization, eventually leading to functional failures [10]. However, whether CLDN-1 functions in the oral epithelium that harbors keratinocytes is not completely understood [11]. Other components of TJs include zonula occludens (ZO) proteins that belong to the membrane-associated guanylate kinase family [12]. ZO-1 binds directly to the C-terminal domain of CLDNs [12] and serves as a linker between CLDNs, the cytoskeleton, and cell signaling pathways [13]. ZO-1 is a member of the family of proteins that localize to adhesion

sites and the nucleus in many cell types such as the epithelial cells of kidney or small intestine origin [14]. However, the expression and functions of ZO-1 in the oral epithelium have not been investigated.

Therefore, in the present study, we determined the expression profiles of the representative TJ molecules CLDN-1 and ZO-1 to determine the roles of TJ molecules in the progression of oral squamous cell carcinoma (SCC).

## 2. Materials and methods

### 2.1. Tissue samples

Surgical specimens resected from 72 patients with oral CIS/SCC were routinely fixed in 10% formalin and embedded in paraffin. After review by two pathologists, we selected specimens that simultaneously contained areas of normal epithelia, foci of epithelial dysplasia, CIS, and/or SCC. The number of patients and total number of foci by the anatomical sites are shown in Supplementary Tables 1 and 2. Serial sections (4-μm thick) were prepared for hematoxylin and eosin staining and immunohistochemistry. The Ethical Board of the Niigata University Graduate School of Medical and Dental Sciences (Oral Life Science) reviewed and approved the experimental protocol for analyzing surgical materials.

### 2.2. Antibodies

The antibodies used were as follows: mouse monoclonal antibody against human CLDN-1 (clone XX7, IgG2a) (Santa Cruz Biotechnology, Inc., Santa Cruz, CA, USA), mouse monoclonal antibody against human ZO-1 (clone ZO1-1A12, IgG1) (Thermo Fisher Scientific Inc., Waltham, MA, USA), mouse monoclonal antibody against β-actin (clone

mAbcam 8226, IgG1) (Abcam plc., Cambridge, UK), mouse monoclonal antibody against keratin (K) 17 (clone E3, IgG2b) (Dako, Glostrup, Denmark), and mouse monoclonal antibody against Ki-67 (clone MIB-1, IgG1) (Dako).

### 2.3. Immunohistochemistry

Immunohistochemical analysis of paraffin sections was performed using the Chem-Mate Envision System (Dako). To analyze CLDN-1 and ZO-1 expression, sections were autoclaved in 10 mM Tris buffer (pH 9.0) containing 1 mM EDTA at 121˚C for 10 min. Primary antibodies were used at the following dilutions: 1:100, K17, Ki-67, and CLDN-1 and 1:50, ZO-1. In the controls, the primary antibodies were replaced with the appropriate pre-immune mouse IgG subclasses (Dako).

### 2.4. Analysis of the expression of TJ molecules

We used representative sections of each case with confirmed foci to determine CLDN-1 and ZO-1 expression levels according to the stained area in the cell border, cytoplasm, or both and separately in the nuclei. Foci occupying ≥10% of stained area were considered positive.

### 2.5. Cells

ZK-1, ZK-2, and MK-1 cells of oral SCC origin were cultured as monolayers in Dulbecco's minimal essential medium (Gibco, Thermo Fisher Scientific Inc.) containing 10% fetal calf serum (Gibco), 50 IU/ml penicillin, and 50 μg/ml streptomycin (Gibco) at 37˚C in a humidified atmosphere containing 5% $CO_2$ and 95% air [15]. When the cells reached 50% or 80% confluence, they were subjected to analysis using reverse transcriptase-polymerase chain reaction (RT-PCR), western blotting, cell fractionation, RNA interference (RNAi), immunofluorescence, and the functional assays described in sections 2.11–2.14.

### 2.6. RNA isolation and RT-PCR

ZK-1, ZK-2, MK-1, and transfected cells cultured in 60-mm dishes were lysed with ISOGEN (Nippon Gene, Tokyo, Japan) to extract total RNA. cDNA was synthesized from 5 μg of each RNA sample using the Invitrogen SuperScript III First-Strand Synthesis System (Thermo Fisher Scientific) followed by PCR. Primer sequences, reaction conditions, and optimal cycle numbers of PCR products for amplifying *CLDN-1*, *ZO-1*, and *GAPDH* DNAs are presented in Supplementary Table 3.

### 2.7. Cell fractionation

Cell fractionations were performed in ZK-1 cell cultures on days 3 and 6 using a Nuclear and Membrane Protein Extraction Kit (NE-PER, Mem-Per plus; Thermo Fisher Scientific) according to the manufacturer's instructions. All proteins extracted from membrane, nuclear, and cytosolic fractions were subjected to western blotting (section 2.9).

### 2.8. RNAi

RNAi experiments were performed using the Stealth RNAi siRNA Duplex Oligoribonucleotides System (Thermo Fisher Scientific) as described in [15], in which we used three different small interference RNA (siRNA) sequences each for *CLDN-1* and *ZO-1* (Supplementary Table 4).

### 2.9. Western blotting

Untransfected and transfected ZK-1 cells were lysed on days 3–6 after seeding, and the cell lysates were subjected to western blotting. The primary antibodies were used at the following dilutions: 1:200, CLDN-1; 1:500, ZO-1; and 1:4000, β-actin. Immunocomplexes were visualized using the ECL Prime Western Blotting Detection System (GE Healthcare UK, Ltd., Little Chalfont, UK).

**2.10. Immunofluorescence**

ZK-1 cells were plated ($1.25 \times 10^4$ cells per well) and cultured for 3 and 6 days in chamber slides. Transfected cells were analyzed on days 3 and 5. The cells were fixed with 4% paraformaldehyde and permeabilized with 0.2% Triton X-100 in phosphate-buffered saline (PBS). After blocking the membranes with 5% skim milk in PBS to prevent nonspecific binding, the cells were incubated with the primary antibodies for 1 h at room temperature, washed, and then incubated with Alexa Fluor 488-conjugated goat anti-mouse IgG (Molecular Probes, Thermo Fisher Scientific). The cells were counterstained with 4′,6-diamidino-2-phenylindole (DAPI) (Dianova, Hamburg, Germany).

**2.11. Growth curve analysis**

ZK-1 cells were transfected with *CLDN-1* siRNA (Csi), *ZO-1* siRNA (Zsi), or scramble siRNA for 48 h. Transfected cells were seeded at $3 \times 10^4$ in 35-mm dishes. On days 1, 3, and 5 after seeding, cells were counted.

**2.12. Apoptosis assay**

Apoptotic cells were detected using flow cytometry with a MEBCYTO Apoptosis Kit (MBL Co., Ltd., Nagoya, Japan). Cells transfected with siRNAs for 48 h were stained with Annexin V-FITC and propidium iodide according to the distributor's protocols. The treated cells were analyzed using a BD FACS Aria II Cell Sorter (BD Biosciences, Franklin Lakes, NJ, USA).

**2.13. Bromodeoxyuridine (BrdU) cell proliferation assay**

The proliferation of cells was determined using CycLex BrdU ELISA Kit (MBL Co., Ltd.) following to the distributor's protocols. Briefly, $1 \times 10^4$ cells were reseeded into a 96-well microplate at day 3 after transfection, and incubated for 12 h. The cells were labeled

with BrdU at a concentration of 10 μM for 2 h. After fixation and denaturation, the plate was incubated with the primary antibody solution, and followed by the secondary antibody solution. The signals were developed with the substrate reagent, and then quantified by measuring the absorbance at 450 nm on a microplate reader.

### 2.14. Cell invasion assay

Invasion of Matrigel (BD Biosciences) using $0.5 \times 10^6$ cells per assay was determined using the BD Falcon Cell Culture Inserts and Companion Plates System (12 wells, 8 μm pore size) (BD Biosciences) as described elsewhere [15]. Insert membranes were coated with Matrigel (BD Biosciences).

### 2.15. Statistical analysis

All experiments were performed in triplicate, and the values from three experiments were averaged and plotted along with standard deviation (SD) values. The data were analyzed by one-way analysis of variance, followed by a post hoc Tukey's multiple comparison test using GraphPad Prism 6 (GraphPad Software, Inc., La Jolla, CA, USA). $P < 0.05$ indicates statistically significant differences.

## 3. Results

### 3.1. Immunohistochemical analysis of the expression of TJ molecules

We categorized epithelial dysplasias and CIS according to the expression of K17 and Ki-67 [16, 17] (Fig. 1). The numbers of foci positive for CLDN-1 and ZO-1 are indicated in Table 1, Supplementary Tables 1, and 2. CLDN-1 was not detected in the epithelial layer of

the normal oral mucosa (Fig. 1A–D). ZO-1 was detected within the cytoplasm of keratinized cells in 5 of 19 foci (26%) of normal epithelial foci (Fig. 1E). In epithelial dysplasia with a two-phase appearance (moderate degree) (Fig. 1F–H), CLDN-1 was detected in the lower half of 12 of 50 foci (24%), although staining intensity was generally weak (Fig. 1I). ZO-1 expression associated with the cell border and cytoplasm was detected in 48 of 50 dysplastic foci (96%), and it was detected in the nucleus in the lower half (Fig. 1J) where proliferating Ki-67-positive (+) cells were detected in 33 of 50 (66%) dysplastic foci (Fig. 1G).

We proposed a system for evaluating the histological variations of oral CIS such as basaloid and differentiated types [16]. Basaloid CIS is characterized by a uniform proliferation of basaloid cells with a narrow cytoplasm and an enlarged nucleus, which is confirmed by the expansion of the population of Ki-67+ cells [16]. Analysis of basaloid CIS (Fig. 1K–M) revealed that CLDN-1 was mainly localized to the borders of CIS cells in the upper half and was distributed diffusely in the cytoplasm of those in the lower half (Fig. 1N). Moreover, ZO-1 staining was more intensely positive in most of the nuclei and in the cytoplasm of the lower half (Fig. 1O) where Ki-67+ cells were abundant and in close proximity to each other (Fig. 1L). In differentiated CIS (Fig. 1P–R), which is characterized by definite keratinization of the surface [17], the intensity of CLDN-1 staining was enhanced in the cell border of the middle-layer zone, showing a characteristic honeycomb pattern (Fig. 1S). In CIS cells, ZO-1 was localized in the nucleus as well as in the cytoplasm of cells in the lower half (Fig. 1T), which was nearly identical to the distribution of Ki-67+ cells (Fig. 1Q). The expression patterns of CLDN-1 and ZO-1 in differentiated CIS were similar to those in basaloid CIS. Consistent with increased detection of CLDN-1 (51 of 53 foci, 96%), ZO-1 was detected in the cell border and cytoplasm of 52 of 53 (98%) CIS foci, and the nuclear localization of ZO-1 was detected in 37 of 53 CIS foci (70%).

In well-differentiated SCC (Fig. 1U–W), CLDN-1 was characteristically demonstrated on the cell border in most of the tumor nests in 34 of 34 foci (100%) (Fig. 1X). ZO-1 was

localized within the nuclei of peripheral cells of the nests in 28 of 34 foci (82%) as well as in their cell border and cytoplasm (Fig. 1Y), which was almost the same as the Ki-67+ cell localization (Fig. 1V). Nuclear localization of CLDN-1was not observed in all of SCC foci as well as normal, dysplastic, and CIS foci. There was no tendency of the anatomical sites in the positivity of CLDN-1 and ZO-1 (Supplementary Tables 1 and 2).

### 3.2. Expression of TJ molecules in cultured oral SCC cells

RT-PCR assays detected equivalent levels of the mRNAs encoding *ZO-1* and *CLDN-1* in ZK-1, ZK-2, and MK-1 cells (Fig. 2A), and western blot analysis of different cell fractions are shown in Fig. 2B. Three days after plating, ZK-1 cells were scattered and covered approximately 50% of the culture dishes, and CLDN-1 was mainly detected in the cytoplasm (Fig. 2B, left). In contrast, ZO-1 was detected in the nucleus and cytoplasm (Fig. 2B, right). On day 6, the ZK-1 cells were densely packed and covered over 80% of the culture dishes. CLDN-1 was detected in the cell membrane of these cells as well as in the cytoplasm, and a faint band was detected in the nucleus (Fig. 2B). In contrast, ZO-1 was mostly concentrated in the cytoplasm (Fig. 2B). Immunofluorescence analyses of ZK-1 cells confirmed these differential patterns of expression (Fig. 2C), which were similar to those in tissue sections of CIS and SCC. We used ZK-1 cells in the following experiments.

### 3.3. Decreased expression of TJ molecules in oral SCC cells

To determine their functions, we inhibited the expression of CLDN-1 and ZO-1 by transfecting ZK-1 cells with their respective cognate siRNAs. RT-PCR analysis demonstrated that the three siRNAs targeting each mRNA were similarly effective in inhibiting the expression of *CLDN-1* and *ZO-1* mRNAs on day 5 after plating (Supplementary Fig. 1). Western blotting detected reduced levels of CLDN-1 and ZO-1 that differed slightly in cells transfected with each of the three siRNAs (Fig. 3A). We selected *CLDN-1* siRNAs (Csi) #1

and #3 and *ZO-1* siRNAs (Zsi) #2 and #3 for the following experiments because they were more effective in inhibiting CLDN-1 and ZO-1 expression, which was indicated by the intensities of the bands detected in western blots. Phase-contrast microscopy revealed the dissociation of the ZK-1 cells transfected with *CLDN-1* siRNAs (Fig. 3B, Csi #1), although their morphology was not affected by the *ZO-1* siRNAs (Fig. 3B, Zsi #3) compared with controls (Fig. 3B, vehicle and scramble).

Immunofluorescence of CLDN-1 on the cell border of controls (Fig. 3C, a, b) was undetectable in Csi #1-ZK-1 cells (Fig. 3C, c). Further, ZO-1 was detected mainly within the cytoplasm, particularly in the perinuclear zone (Fig. 3C, g). ZO-1 immunofluorescence was undetectable in Zsi #3-ZK-1 cells (Fig. 3C, h), and CLDN-1 signals were distributed diffusely in the cytoplasm but only partially on the cell border (Fig. 3C, d). The inhibitory effects of Csi #2/#3 and Zsi #1/#2 were diminished compared with those of Csi #1 and Zsi #3, respectively (Supplementary Fig. 2).

Csi #1/#3 (Fig. 4A) and Zsi #3 (Fig. 4B) significantly inhibited the growth of ZK-1 cells on day 5, which was confirmed by the results of BrdU cell proliferation assay (Fig. 4C). In contrast, the decreased number of cells transfected with Zsi #2 was not statistically significant compared with the control. This finding corresponds to the results of the immunofluorescence assays showing that the expression pattern of CLDN-1 in Zsi #2 cells was not significantly inhibited (Supplementary Fig. 2). Apoptosis assays did not detect a difference in death between the Csi/Zsi-transfected cells and the controls (Supplementary Fig. 3).

Matrigel assays showed that the invasion by ZK-1 cells was significantly decreased by Csi #1 and Csi #3 (Fig. 4D) as well as by Zsi #2 and Zsi #3 (Fig. 4E). Thus, the invasiveness of ZK-1 cells correlated with the expression levels of these two TJ molecules.

## 4. Discussion

In the present study, we showed for the first time that stepwise overexpression of CLDN-1 and ZO-1 in oral malignancies such as epithelial dysplasia, CIS, and SCC, together with their mutually dependent functions, contributes to the proliferation and invasiveness of oral SCC cells.

Here we detected CLDN-1 and ZO-1 in oral malignancies but not in the normal oral epithelium. Our results indicated that CLDN-1 expression was enhanced in most oral CIS and SCC and are consistent with other reports [11, 18–22]. Ouban et al. reported differential pattern of CLDN-1 expression among tumors of different anatomical sites [22]. However, our observation indicated that there were no obvious influences of the anatomical location to the expression pattern of CLDN-1. Overexpression of CLDN-1 occurs in cancers of other organs such as the colon [6, 23]. We show here that CLDN-1 expression in the cell border was localized above the middle layer of CIS (Fig. 1N, S), which is the site of β-catenin translocation to the nucleus [4]. This finding is consistent with a report that transcription of *CLDN-1* is increased by the β-catenin/TCF4 complex in colon cancer [24]. Moreover, we show here that CLDN-1 expression was undetectable in normal oral epithelia, although others found that CLDN-1 is expressed in normal epithelia as well as in SCC [11, 19, 25]. However, their figures that show normal epithelia appear to show neoplastic change.

To our knowledge, the present study is the first to determine the expression pattern of ZO-1 in oral mucosal epithelia in normal and neoplastic conditions. In normal oral epithelia, ZO-1 was occasionally positive within the cytoplasm of keratinized cells in the parakeratotic layer (Fig. 1E). This differs from the data for the epidermis showing that ZO-1 is localized to the cell border of the granular and upper prickle-cell layer [26] as well as the esophageal mucosa, in which a punctate pattern of expression of ZO-1 is observed in the cell border of the superficial layer [27]. In Bowen's disease and SCC of the skin, ZO-1 and CLDNs are strongly expressed in keratinizing cancer cells [26], suggesting that TJ is associated with

keratinization. In the oral malignancies analyzed here, upregulation of ZO-1 expression was detected in the nucleus as well as in the cell border (Fig. 1J, O, T, Y) and was accompanied by increased CLDN-1 expression. From our immunohistochemical analysis, we conclude that the presence of CLDN-1 in the cell membrane and the presence of ZO-1 in the nucleus serve as hallmarks of oral malignancies.

TJ serves as a cell adhesion apparatus as well as a multifunctional apparatus that mediates cell proliferation and invasion [5-7]. TJ molecules play important roles in the proliferation of oral SCC cells because both CLDN-1 and ZO-1 regulated the growth of oral SCC cells, as indicated by the results of the RNAi experiments (Fig. 4A–C). Increased expression of CLDN-1 inhibits apoptosis, which sustains cell proliferation in nasopharyngeal carcinoma cells [28]. However, inhibition of CLDN-1 or ZO-1 expression had no significant effects on the death of oral SCC cells (Supplementary Fig. 3). Thus, both proteins may contribute to the maintenance of cell proliferation. At present, little is known about how CLDN-1 overexpression contributes to cell proliferation. ZO-1 has reciprocal functions in cell proliferation. That is, ZO-1 inhibits the proliferation since ZO-1 anchors ZO-1-associated nucleic acid binding protein (ZONAB) in the cytoplasm. ZONAB regulates the transcription of genes that are important for G1/S-phase progression including cyclin D1 [29]. In contrast, ZO-1 promotes the proliferation of renal collecting duct cells by inhibiting the expression of cyclin-dependent kinase inhibitor 1 [30]. The detection here of ZO-1 in the nucleus of proliferating Ki-67+ cells in oral epithelial dysplasia and CIS/SCC suggests a crucial role of ZO-1 in the development and growth of oral SCC, although further studies are needed to understand the roles of TJ molecules in cell proliferation.

TJ molecules regulate tumor invasion, and the loss of cellular adhesion, including TJs, leads to invasive growth through the epithelial-mesenchymal transition (EMT) [6]. However, overexpression of TJ molecules paradoxically drives tumor progression and metastasis [31]. We show here that inhibiting the expression of CLDN-1 induced cells to dissociate (Fig. 3B)

but decreased the invasiveness of SCC cells (Fig. 4D), which is consistent with other studies [11, 32]. Oku et al. demonstrated that increased expression of CLDN-1 is associated with MMP-2 activation, MMP-14 expression, and cleavage of laminin-5γ2 [32], indicating that CLDN-1 leads ECM remodeling in the tumor microenvironment to initiate invasion. Suh et al. reported that CLDN-1 induces EMT through the upregulation of the transcription factors SLUG and ZEB1 and thus enhances the invasiveness of cells derived from normal human liver and hepatocellular carcinomas [33]. Moreover, we show here that the invasiveness of oral SCC cells is regulated by ZO-1 (Fig. 4E). Further, ZO-1 reportedly controls the invasiveness of human mammary carcinoma cells in an MMP-14-dependent manner [34].

The localizations of CLDN-1 and ZO-1 are likely dependent on their expression levels. We show here that that the localization of CLDN-1 in the cell border was dependent on ZO-1 (Fig. 3C, d), suggesting that ZO-1 regulates the assembly of CLDN-1 into the cell membrane. This result is consistent with a report that polymerization of CLDNs is altered in epithelial cells that do not express ZO proteins [12]. Further, localization of ZO-1 at the cell border was not detected in cells transfected with *CLDN-1* siRNAs (Fig. 3C, g), indicating that the incorporation of ZO-1 into TJs is likely dependent on prior integration of CLDN-1 into the cell membrane.

Recent evidence indicates an interaction between TJ molecules and keratins, which are cytoskeletal filaments mainly found in cells of epithelial origin. Mutations in K18 gene cause abnormal distribution of ZO-1 and CLDN-4 in cultured colonocytes impair intestinal barrier function [35]. In contrast, Fortier et al. reported that loss of K8/K18 in cancer cells enhances their motility and invasion through the activation of the PI3K/AKT pathway and transactivation of *CLDN*-1 by NF-κB [36]. Our present study shows that aberrant expression of CLDN-1 and ZO-1 coincided with the expression of K17 in oral SCC/CIS (Fig. 1H, M, R, W). We previously reported keratin-subtype switching from K13 to K17 during the neoplastic transformation of oral mucosal epithelial cells [17], which leads to increased cell proliferation

induced by the interaction of K17 with 14-3-3 sigma [37]. However, direct interaction between TJ molecules and keratins remains to be clarified.

In conclusion, the findings of the present study provide a strong foundation for identifying the molecular mechanisms of the coincident activities of cytoskeletal components and TJ molecules associated with the malignant transformation of oral epithelial cells. Moreover, because TJs are essential for the growth and invasive properties of oral SCC cells, they should serve as a novel immunohistochemical marker for diagnosing oral borderline malignancies. Our findings emphasize the importance of identifying the molecular mechanisms underlying the aberrant expression of TJ molecules. Further, TJ molecules may serve as novel targets for cancer therapy, as CLDN-1 can be an epitope recognized by cytotoxic T lymphocytes [38].

## Acknowledgments

This work was supported in part by Grants-in-Aid for Scientific Research from the Japan Society for the Promotion of Science (JSPS KAKENHI grant nos. 25305035 and 25462849 to J. C. and 26305032 and 15K15693 to T. S.) and by a scholarship from the Government of Saudi Arabia (H. B.). We thank Dr. Hiroko Kato and Prof. Kenji Izumi for their valuable cooperation in helping us perform the apoptosis assay.

## References


[1] van Dijk M, Goransson SA, Stromblad S. Cell to extracellular matrix interactions and their reciprocal nature in cancer. Exp Cell Res 2013; 319, 1663-70.

[2] Schmalhofer O, Brabletz S, Brabletz T. E-cadherin, beta-catenin, and ZEB1 in malignant progression of cancer. Cancer Metastasis Rev 2009; 28, 151-66.

[3] McCrea PD, Gu D, Balda MS. Junctional music that the nucleus hears: cell-cell contact signaling and the modulation of gene activity. Cold Spring Harb Perspect Biol 2009; 1, a002923.

[4] Alvarado CG, Maruyama S, Cheng J, et al. Nuclear translocation of beta-catenin synchronized with loss of E-cadherin in oral epithelial dysplasia with a characteristic two-phase appearance. Histopathology 2011; 59, 283-91.

[5] Tsukita S, Yamazaki Y, Katsuno T, Tamura A, Tsukita S. Tight junction-based epithelial microenvironment and cell proliferation. Oncogene 2008; 27, 6930-8.

[6] Sawada N. Tight junction-related human diseases. Pathol Int 2013; 63, 1-12.

[7] Schneeberger EE, Lynch RD. The tight junction: a multifunctional complex. Am J Physiol Cell Physiol 2004; 286, C1213-28.

[8] Schlüter H, Moll I, Wolburg H, Franke WW. The different structures containing tight junction proteins in epidermal and other stratified epithelial cells, including squamous cell metaplasia. Eur J Cell Biol 2007; 86, 645-55.

[9] Myal Y, Leygue E, Blanchard AA. Claudin 1 in breast tumorigenesis: revelation of a possible novel "claudin high" subset of breast cancers. J Biomed Biotechnol 2010; 2010, 956897.

[10] Sugawara T, Iwamoto N, Akashi M, et al. Tight junction dysfunction in the stratum granulosum leads to aberrant stratum corneum barrier function in claudin-1-deficient mice. J Dermatol Sci 2013; 70, 12-8.

[11] dos Reis PP, Bharadwaj RR, Machado J, et al. Claudin 1 overexpression increases invasion and is associated with aggressive histological features in oral squamous cell carcinoma. Cancer 2008; 113, 3169-80.

[12] Umeda K, Ikenouchi J, Katahira-Tayama S, et al. ZO-1 and ZO-2 independently determine where claudins are polymerized in tight-junction strand formation. Cell 2006; 126, 741-54.

[13] Siljamaki E, Raiko L, Toriseva M, et al. p38delta mitogen-activated protein kinase regulates the expression of tight junction protein ZO-1 in differentiating human epidermal keratinocytes. Arch Dermatol Res 2014; 306, 131-41.

[14] Gottardi CJ, Arpin M, Fanning AS, Louvard D. The junction-associated protein, zonula occludens-1, localizes to the nucleus before the maturation and during the remodeling of cell-cell contacts. Proc Natl Acad Sci U S A 1996; 93, 10779-84.

[15] Yamazaki M, Maruyama S, Abé T, et al. MFG-E8 expression for progression of oral squamous cell carcinoma and for self-clearance of apoptotic cells. Lab Invest 2014; 94, 1260-72.

[16] Kobayashi T, Maruyama S, Cheng J, et al. Histopathological varieties of oral carcinoma in situ: Diagnosis aided by immunohistochemistry dealing with the second basal cell layer as the proliferating center of oral mucosal epithelia. Pathol Int 2010; 60, 156-66.

[17] Mikami T, Cheng J, Maruyama S, et al. Emergence of keratin 17 vs. loss of keratin 13: their reciprocal immunohistochemical profiles in oral carcinoma in situ. Oral Oncol 2011; 47, 497-503.

[18] Bello IO, Vilen ST, Niinimaa A, et al. Expression of claudins 1, 4, 5, and 7 and occludin, and relationship with prognosis in squamous cell carcinoma of the tongue. Hum Pathol 2008; 39, 1212-20.

[19] Lourenço SV, Coutinho-Camillo CM, Buim ME, et al. Oral squamous cell carcinoma: status of tight junction claudins in the different histopathological patterns and relationship with clinical parameters. A tissue-microarray-based study of 136 cases. J Clin Pathol 2010; 63, 609-14.

[20] Sappayatosok K, Phattarataratip E. Overexpression of Claudin-1 is Associated with Advanced Clinical Stage and Invasive Pathologic Characteristics of Oral Squamous Cell Carcinoma. Head Neck Pathol 2015; 9, 173-80.

[21] Ouban A, Hamdan H, Hakam A, Ahmed AA. Claudin-1 expression in squamous cell carcinomas of different organs: comparative study of cancerous tissues and normal controls. Int J Surg Pathol 2012; 20, 132-8.

[22] Ouban A, Ahmed A. Analysis of the distribution and expression of claudin-1 tight junction protein in the oral cavity. Appl Immunohistochem Mol Morphol 2015; 23, 444-8.

[23] Dhawan P, Singh AB, Deane NG, et al. Claudin-1 regulates cellular transformation and metastatic behavior in colon cancer. J Clin Invest 2005; 115, 1765-76.

[24] Miwa N, Furuse M, Tsukita S, et al. Involvement of claudin-1 in the beta-catenin/Tcf signaling pathway and its frequent upregulation in human colorectal cancers. Oncol Res 2001; 12, 469-76.

[25] Nelhűbel GA, Károly B, Szabó B, et al. The prognostic role of claudins in head and neck squamous cell carcinomas. Pathol Oncol Res 2014; 20, 99-106.

[26] Morita K, Tsukita S, Miyachi Y. Tight junction-associated proteins (occludin, ZO-1, claudin-1, claudin-4) in squamous cell carcinoma and Bowen's disease. Br J Dermatol 2004; 151, 328-34.

[27] Oshima T, Koseki J, Chen X, Matsumoto T, Miwa H. Acid modulates the squamous epithelial barrier function by modulating the localization of claudins in the superficial layers. Lab Invest 2012; 92, 22-31.

[28] Lee JW, Hsiao WT, Chen HY, et al. Upregulated claudin-1 expression confers resistance to cell death of nasopharyngeal carcinoma cells. Int J Cancer 2010; 126, 1353-66.

[29] Sourisseau T, Georgiadis A, Tsapara A, et al. Regulation of PCNA and cyclin D1 expression and epithelial morphogenesis by the ZO-1-regulated transcription factor ZONAB/DbpA. Mol Cell Biol 2006; 26, 2387-98.

[30] Qiao X, Roth I, Feraille E, Hasler U. Different effects of ZO-1, ZO-2 and ZO-3 silencing on kidney collecting duct principal cell proliferation and adhesion. Cell Cycle 2014; 13, 3059-75.

[31] Leech AO, Cruz RG, Hill AD, Hopkins AM. Paradigms lost-an emerging role for over-expression of tight junction adhesion proteins in cancer pathogenesis. Ann Transl Med 2015; 3, 184.

[32] Oku N, Sasabe E, Ueta E, Yamamoto T, Osaki T. Tight junction protein claudin-1 enhances the invasive activity of oral squamous cell carcinoma cells by promoting cleavage of laminin-5 gamma2 chain via matrix metalloproteinase (MMP)-2 and membrane-type MMP-1. Cancer Res 2006; 66, 5251-7.

[33] Suh Y, Yoon CH, Kim RK, et al. Claudin-1 induces epithelial-mesenchymal transition through activation of the c-Abl-ERK signaling pathway in human liver cells. Oncogene 2013; 32, 4873-82.

[34] Polette M, Mestdagt M, Bindels S, et al. Beta-catenin and ZO-1: shuttle molecules involved in tumor invasion-associated epithelial-mesenchymal transition processes. Cells Tissues Organs 2007; 185, 61-5.

[35] Zupancic T, Stojan J, Lane EB, et al. Intestinal cell barrier function in vitro is severely compromised by keratin 8 and 18 mutations identified in patients with inflammatory bowel disease. PLoS One 2014; 9, e99398.

[36] Fortier AM, Asselin E, Cadrin M. Keratin 8 and 18 loss in epithelial cancer cells increases collective cell migration and cisplatin sensitivity through claudin1 up-regulation. J Biol Chem 2013; 288, 11555-71.

[37] Mikami T, Maruyama S, Abé T, et al. Keratin 17 is co-expressed with 14-3-3 sigma in oral carcinoma in situ and squamous cell carcinoma and modulates cell proliferation and size but not cell migration. Virchows Arch 2015; 466, 559-69.

[38] Kondo S, Demachi-Okamura A, Hirosawa T, et al. An HLA-modified ovarian cancer cell line induced CTL responses specific to an epitope derived from claudin-1 presented by HLA-A*24:02 molecules. Hum Immunol 2013; 74, 1103-10.

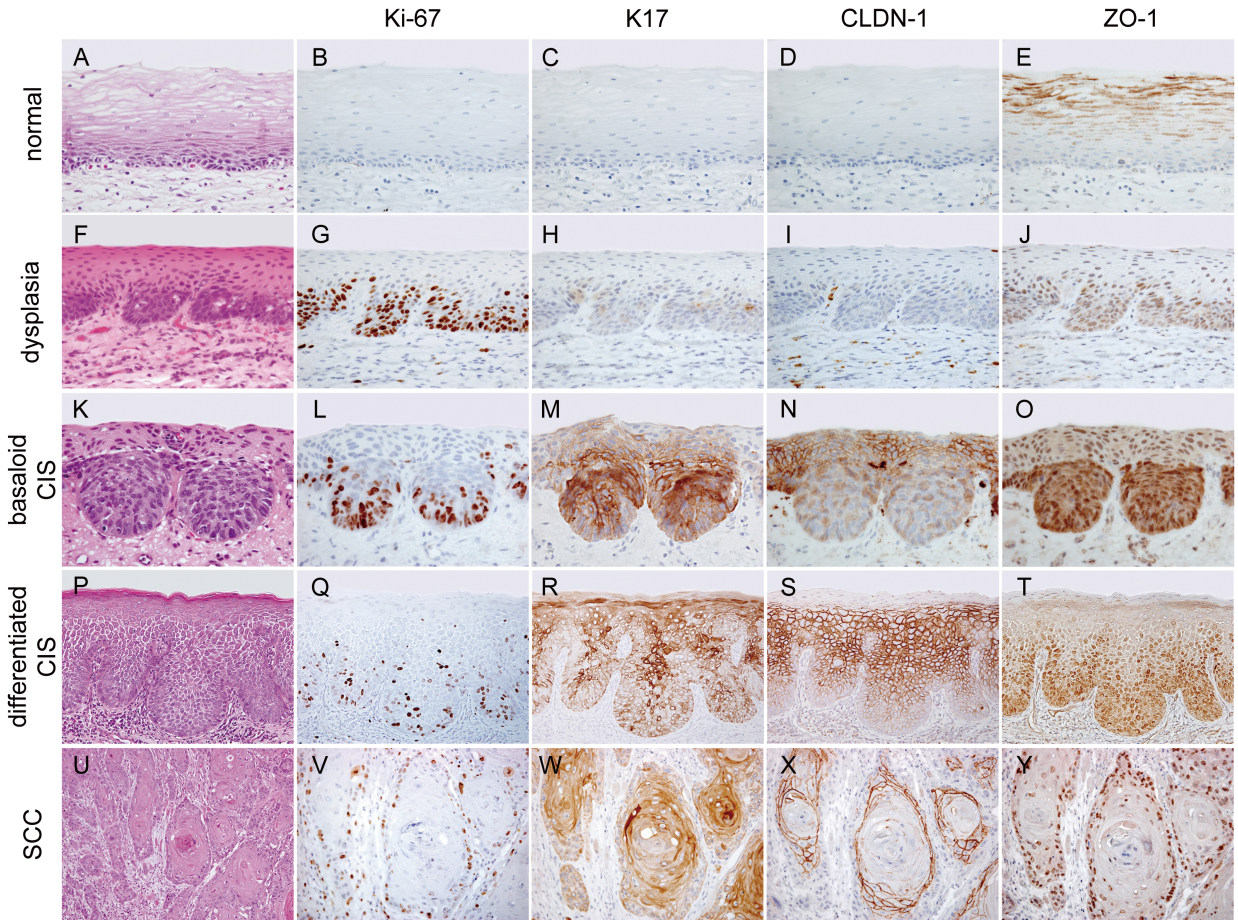


**Fig. 1 Immunohistochemical expression profiles of tight junction (TJ) molecules in the normal oral mucosa, epithelial dysplasia, carcinoma in-situ (CIS), and squamous cell carcinoma (SCC).** Normal epithelia (A–E), epithelial dysplasia (F–J), basaloid CIS (K–O), differentiated CIS (P–T), and SCC (U–Y). Hematoxylin and eosin stain (A, F, K, P, U); immunoperoxidase stains to detect Ki-67 (B, G, L, Q, V), keratin (K) 17 (C, H, M, R, W), claudin-1 (CLDN-1) (D, I, N, S, X) and zonula occludens-1 (ZO-1) (E, J, O, T, Y), hematoxylin counterstain. Original magnifications × 400 (A–J), × 600 (K–O); × 200 (P–T, V–Y); × 100 (U).

In normal epithelia (A), CLDN-1 was not detected in the epithelial layer (D). ZO-1 was occasionally positive within the cytoplasm of keratinized cells (E). In epithelial dysplasia with a two-phase appearance (F), proliferating cells tested for Ki-67 were condensed in the lower half (G), their nuclei were positive for ZO-1 (J). In basaloid CIS (K), in which large Ki-67-positive nuclei were accumulated in the basal zone (L), CLDN-1 was localized mainly to the cell borders of CIS cells in the upper half as well as diffusely in the cytoplasm of those in the lower half (N). ZO-1 was more intensely positive in most of the nuclei and in the cytoplasm of the lower half (O). In differentiated CIS (P), CLDN-1 expression was enhanced in the border of the prickle-cell layer, which showed a characteristic honeycomb pattern (S). In contrast, ZO-1 was localized in the nuclei of CIS cells and in the cytoplasm of the cells in the lower-half (T). In well-differentiated SCC (U), CLDN-1 was characteristically detected on the cell border of SCC cells in the peripheral to middle zones of foci (X), whereas ZO-1 was localized within the nuclei of the basal cells of SCC foci (Y), which was similar to the location of Ki-67-positive cells.

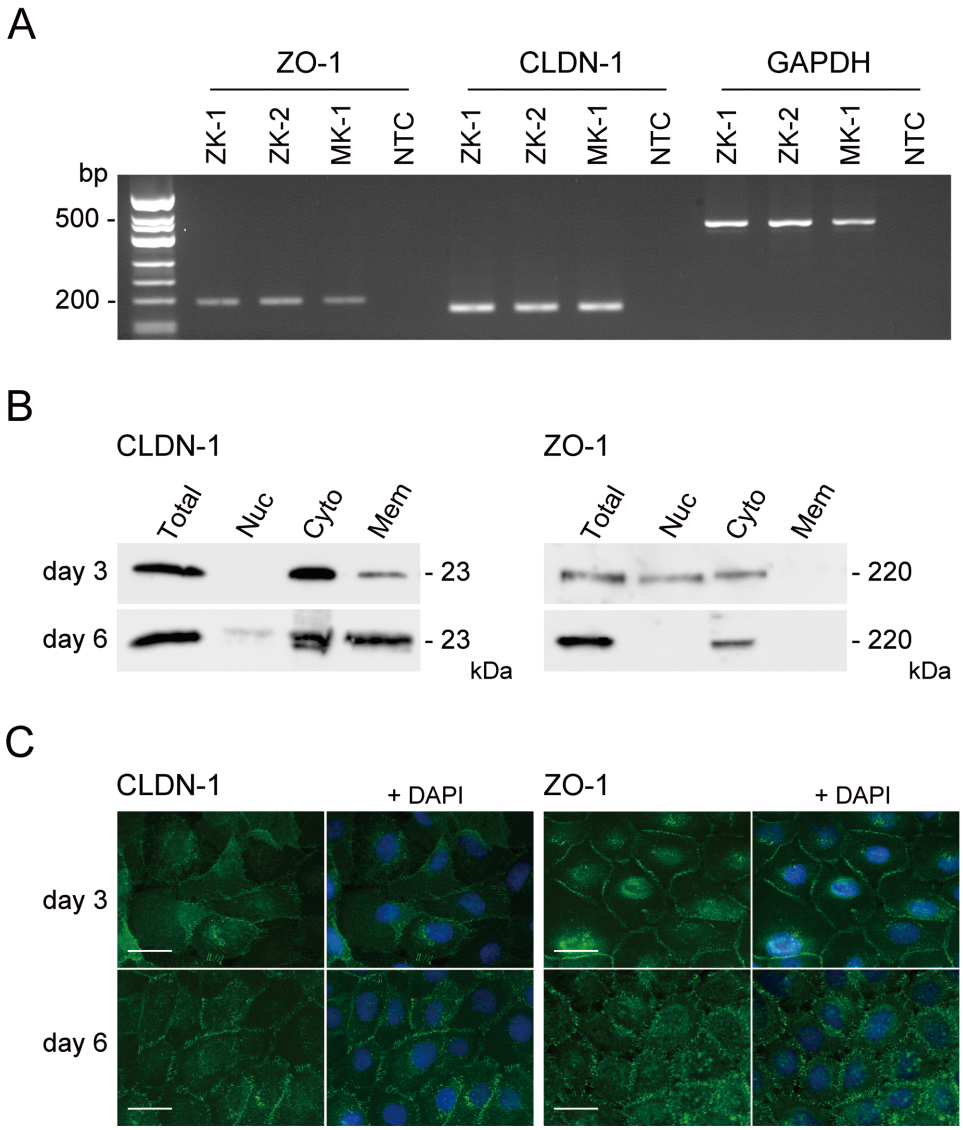


**Fig. 2 Expression of the genes encoding TJ molecules in cultured SCC cells.** A, Reverse transcriptase-polymerase chain reaction (RT-PCR) analysis of ZO-1 (left), CLDN-1 (middle), and GAPDH (right) mRNAs in ZK-1, ZK-2, MK-1 cells, and no template control (NTC). Agarose gel (3%) electrophoresis. B, Western blotting analysis of the expression of CLDN-1 (left) and ZO-1 (right) in four cell fractions of ZK-1 cells cultivated for 3 and 6 days. Abbreviations: total cell lysate (Total), nucleus (Nuc), cytoplasm (Cyto), and cell membrane (Mem). C, Immunofluorescence analysis of the expression of CLDN-1 (left column, second left) and ZO-1 (right, second right) in ZK-1 cells without or with DAPI (blue) on days 3 (upper) and 6 (lower). Scale bar = 25 μm.

RT-PCR analysis detected the expression of ZO-1 and CLDN-1 mRNAs in three SCC cell lines (A). Western blotting showed that CLDN-1 was mainly concentrated in the cell membrane and in the cytoplasm (B, left panel). In contrast, ZO-1 was detected in the nucleus and cytoplasm on day 3 but was undetectable in the nucleus on day 6 (B, right). These findings were confirmed using immunofluorescence assays as follows: CLDN-1 signals were mainly localized along the cell border of ZK-1 cells on days 3 and 6 (C, upper and lower left). ZO-1 was clearly localized within the nuclei as well as in the cell border or perinuclear zones on day 3 (C, upper right), although nuclear ZO-1 was undetectable on day 6 (C, lower right).

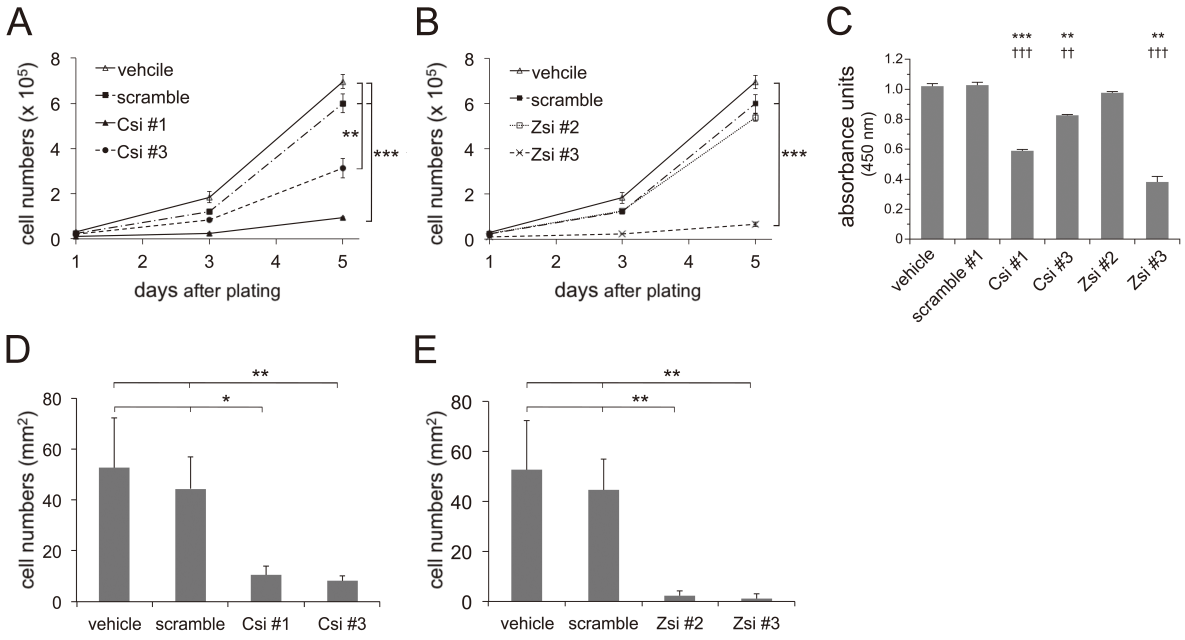


**Fig.4 Cell growth and invasion assays of ZK-1 cells transfected with CLDN-1 or ZO-1 mRNAs.** A, Growth curves of transfected ZK-1 cells. Vehicle (open triangles), scramble (closed squares), CLDN-1 siRNA (Csi) #1 (closed triangles), and Csi #3 (closed circles). B, The growth of ZK-1 cells transfected with ZO-1 siRNAs. Vehicle (open triangles), scramble (closed squares), ZO-1 siRNA (Zsi) #2 (open squares), and Zsi #3 (crosses). C, Bromodeoxyuridine (BrdU) cell proliferation assay of transfected ZK-1 cells. Results were exxpressed as absorbance units at 450 nm. Mean ± SD of triplicate experiments. **P < 0.01, ***P < 0.001 vs. vehicle, ††P < 0.01, †††P < 0.001 vs. scramble #1. D, E, Invasion assays of ZK-1 cells transfected with CLDN-1 or ZO-1 siRNAs. Cell counts per mm2 at 24 h. Mean ± SD of triplicate experiments. *P < 0.05, **P < 0.01, ***P < 0.001.

Transfection with Csi #1 significantly inhibited the growth of ZK-1 cell growth on days 3 ($P < 0.001$) and day 5 ($P < 0.001$). The inhibition caused by Csi #3 was significant on day 5 ($P = 0.001$) (A). Zsi #3 significantly inhibited the growth of ZK-1 cells on days 3 ($P < 0.001$) and 5 ($P < 0.001$), whereas Zsi #2 did not significantly affect the cell growth (B). Measurement of DNA synthesis based on BrdU incorporation indicated that cell proliferation was significantly decreased in the cells transfected with Csi #1, Csi #3, and Zsi #3 (C). In invasion assays, the number of ZK-1 cells decreased significantly when they were transfected with Csi #1 ($P = 0.01$) and Csi #3 ($P = 0.007$) (D). Zsi #2 and Zsi #3 significantly inhibited the invasion of Matrigel by ZK-1 ($P = 0.003$ and $P = 0.003$, respectively) (E).

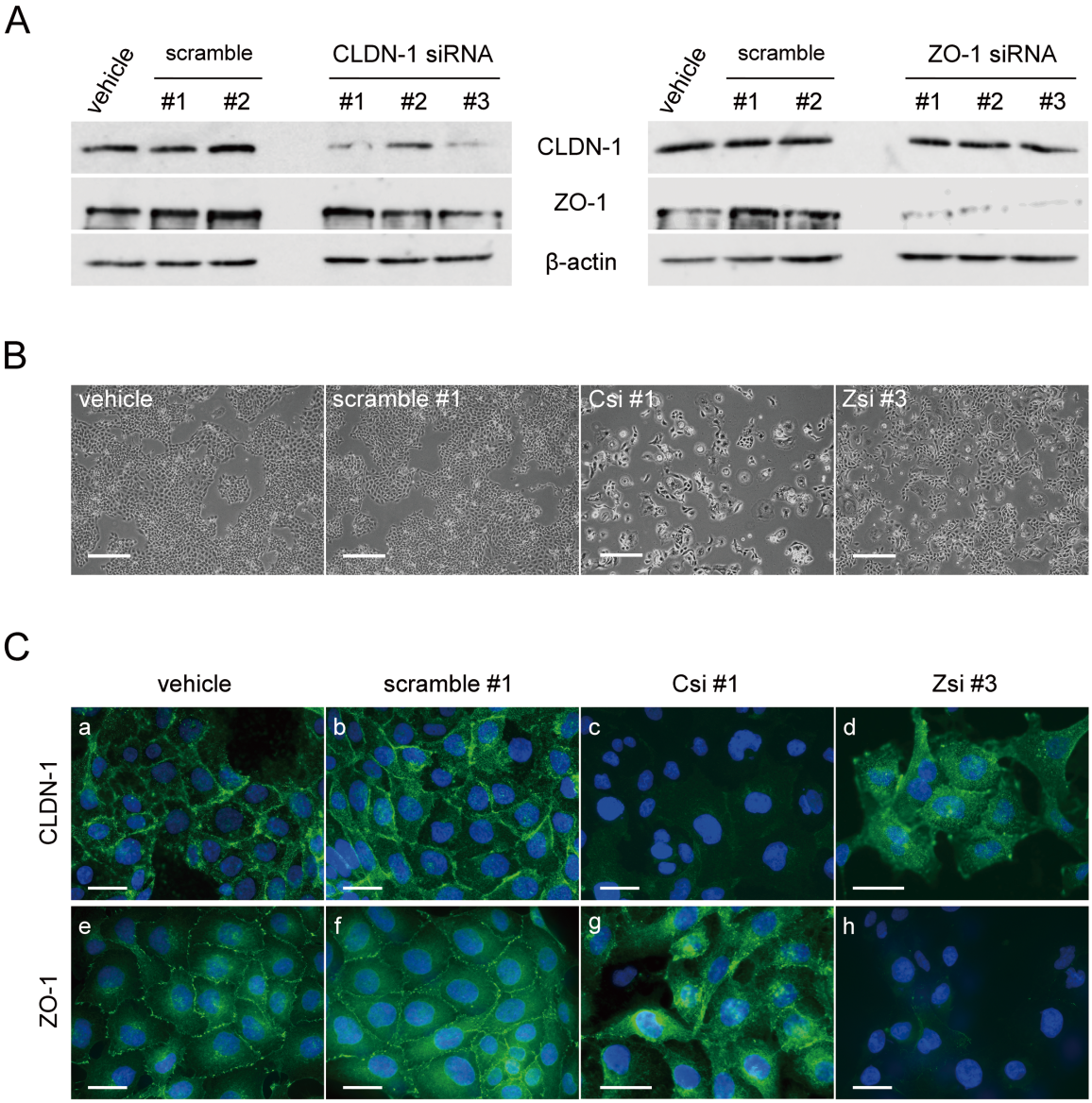


**Fig.3 Inhibition of the expression of genes endoding TJ proteins.** A, Protein levels determined using western blotting in ZK-1 cells transfected with CLDN-1 siRNA (left) or ZO-1 (right) on day 5. Vehicle, scramble RNAs (#1 and #2), siRNAs (#1, #2 and #3) specific for CLDN-1 and ZO-1. B, Phase-contrast images of ZK-1 cells on day 5 after transfection. Controls (vehicle and scramble RNA #1), CLDN-1 siRNA (Csi) #1, and ZO-1 siRNA (Zsi) #3. Scale bar = 500 μm. C, Immunofluorescence analysis of the expression of CLDN-1 (upper) and ZO-1 (lower) in ZK-1 cells cultivated for 3 days after transfection that were counterstained with DAPI (blue). Vehicles (a, e), scramble #1 (b, f), Csi #1 (c, g), Zsi #3 (d, h). Scale bar = 25 μm.

Western blot analysis confirmed the inhibition of CLDN-1 (A; left, upper) and ZO-1 (A; right, middle) expression. Phase-contrast images show the dissociation of ZK-1 cells transfected with Csi #1, whereas cells transfected with Zsi #3 and the controls were not affected (B). CLDN-1 was not detected in cells transfected with Csi #1 (C, c), in which ZO-1 was localized within the cytoplasm, particularly in the perinuclear zone, but not on the cell border (C, g). The expression of ZO-1 was greatly reduced in cells transfected with Zsi #3 (C, h), in which CLDN-1 signals were diffuse in the cytoplasm and were not detected across the entirety of the cell border (C, d).

**Supplementary Table 1.** Immunohistochemical analysis of CLDN-1 by the anatomical sites

| | # of patients | # of CLDN-1 positive foci | | | | | | | |
|---|---|---|---|---|---|---|---|---|---|
| | | normal | | dysplasia | | CIS | | SCC | |
| site | | CB/Cyto | Nuc | CB/Cyto | Nuc | CB/Cyto | Nuc | CB/Cyto | Nuc |
| tongue | 44 | 0/16 (0%) | 0/16 (0%) | 4/33 (12%) | 0/33 (0%) | 31/31 (100%) | 0/31 (0%) | 23/23 (100%) | 0/23 (0%) |
| buccal mucosa | 15 | 0/1 (0%) | 0/1 (0%) | 4/7 (57%) | 0/7 (0%) | 11/13 (85%) | 0/13 (0%) | 6/6 (100%) | 0/6 (0%) |
| floor of the mouth | 7 | 0/1 (0%) | 0/1 (0%) | 2/6 (33%) | 0/6 (0%) | 5/5 (100%) | 0/5 (0%) | 2/2 (100%) | 0/2 (0%) |
| gingiva | 5 | 0/1 (0%) | 0/1 (0%) | 1/3 (33%) | 0/3 (0%) | 3/3 (100%) | 0/3 (0%) | 2/2 (100%) | 0/2 (0%) |
| soft palate | 1 | NA | NA | 1/1 (100%) | 0/1 (0%) | 1/1 (100%) | 0/1 (0%) | 1/1 (100%) | 0/1 (0%) |
| total | 72 | 0/19 (0%) | 0/19 (0%) | 12/50 (24%) | 0/50 (0%) | 51/53 (96%) | 0/53 (0%) | 34/34 (100%) | 0/34 (0%) |

Abbreviations: CB/Cyto, cell border and/or cytoplasm; Nuc, nucleus; CIS, carcinoma in-situ; SCC, squamous cell carcinoma.

**Supplementary Table 2.** Immunohistochemical analysis of ZO-1 by the anatomical sites

| | # of patients | # of ZO-1 positive foci | | | | | | | |
|---|---|---|---|---|---|---|---|---|---|
| | | normal | | dysplasia | | CIS | | SCC | |
| site | | CB/Cyto | Nuc | CB/Cyto | Nuc | CB/Cyto | Nuc | CB/Cyto | Nuc |
| tongue | 44 | 4/16 (25%) | 0/16 (0%) | 33/33 (100%) | 26/33 (79%) | 31/31 (100%) | 23/31 (74%) | 23/23 (100%) | 20/23 (87%) |
| buccal mucosa | 15 | 1/1 (100%) | 0/1 (0%) | 6/7 (86%) | 3/7 (43%) | 13/13 (100%) | 8/14 (57%) | 6/6 (100%) | 4/6 (67%) |
| floor of the mouth | 7 | 0/1 (0%) | 0/1 (0%) | 5/6 (83%) | 2/6 (33%) | 4/5 (67%) | 4/5 (67%) | 2/2 (100%) | 2/2 (100%) |
| gingiva | 5 | 0/1 (0%) | 0/1 (0%) | 3/3 (100%) | 1/3 (33%) | 3/3 (100%) | 2/3 (66%) | 2/2 (100%) | 1/2 (50%) |
| soft palate | 1 | NA | NA | 1/1 (100%) | 1/1 (100%) | 1/1 (100%) | 1/1 (100%) | 1/1 (100%) | 1/1 (100%) |
| total | 72 | 5/19 (26%) | 0/19 (0%) | 48/50 (96%) | 33/50 (66%) | 52/53 (98%) | 37/53 (70%) | 34/34 (100%) | 28/34 (82%) |

Abbreviations: CB/Cyto, cell border and/or cytoplasm; Nuc, nucleus; CIS, carcinoma in-situ; SCC, squamous cell carcinoma.

**Supplementary Table 3.** Primer sets and PCR conditions for *CLDN-1* and *ZO-1*

| Gene | Primer sequence | | Annealing temperature (°C) | Cycle numbers |
|---|---|---|---|---|
| *CLDN-1* | | | | |
| | Forward: | 5′-CGATG AGGTG CAGAA GATGA-3′ | 60 | 27 |
| | Reverse: | 5′-CCAGT GAAGA GAGCC TGACC-3′ | | |
| *ZO-1* | | | | |
| | Forward: | 5′-GCAGC TAGCC AGTGT ACAGT ATAC-3’ | 60 | 32 |
| | Reverse: | 5′-GCCTC AGAAA TCCAG CTTCT CGAA-3′ | | |
| *GAPDH* | | | | |
| | Forward: | 5'-TGAAG GTCGG AGTCA ACGGA TTTGG T-3' | 60 | 30 |
| | Reverse: | 5'-CATGT GGGCC ATGAG GTCCA CCAC-3' | | |

**Supplementary Table 4.** siRNA sequences targeting *CLDN-1* and *ZO-1* genes

| siRNA for | | Sequence |
|---|---|---|
| *CLDN-1* | | |
| | #1 | 5'-CCACA GCAUG GUAUG GCAAU AGAAU-3' |
| | #2 | 5'-CCGGG CAGAU CCAGU GCAAA GUCUU-3' |
| | #3 | 5'-UGCAG AAGAU GAGGA UGGCU GUCAU-'3 |
| *ZO-1* | | |
| | #1 | 5'-GCAGC UCCAA GAGAA AUCUU CGAAA-'3 |
| | #2 | 5'-GGCAA GAGAA GAACC AGAUA UUUAU-'3 |
| | #3 | 5'-CCCUG GAUUU AAGCC AGCCU CUCAA-'3 |

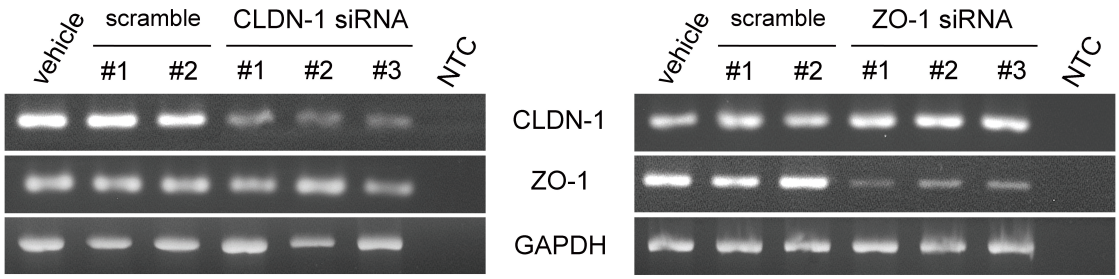


**Supplementary Figure 1.** mRNA expression levels by RT-PCR in *CLDN-1* siRNA (left) and *ZO-1* siRNA (right): vehicle, scramble RNAs (#1 and #2), siRNAs (#1, #2 and #3) for CLDN-1, ZO-1, and no template control (NTC).
RT-PCR demonstrated that three siRNAs were differently effective in suppression for CLDN-1 (left panel, upper row) and ZO-1 (right, middle).

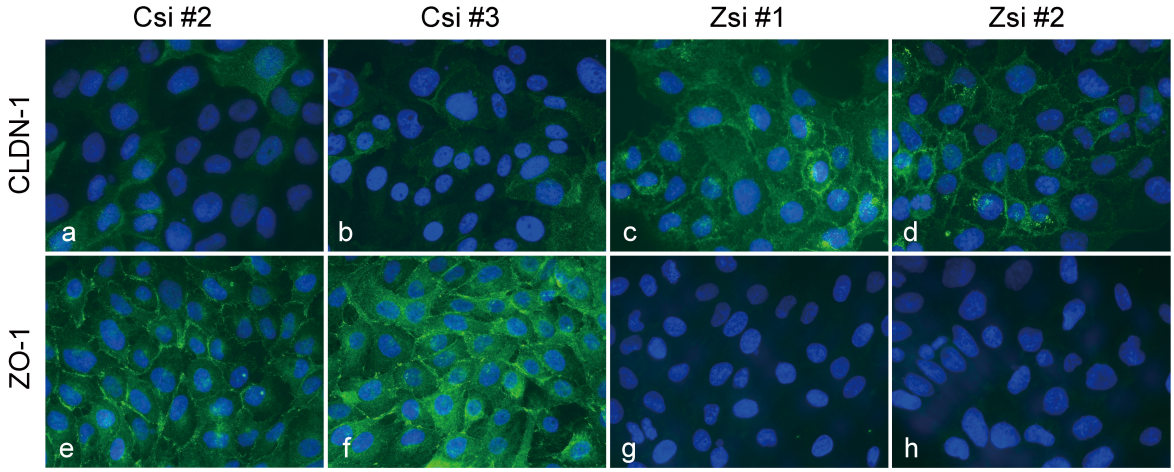


**Supplementary Figure 2.** Immunofluorescence for CLDN-1 (upper, a-d) and ZO-1 (lower, e-h) in TJ gene-suppressed ZK-1 cells cultivated for 3 days, counterstain with DAPI (blue). (a, e) Csi #2, (b, f) Csi #3, (c, g) Zsi #1, and (d, h) Zsi #2.
For CLDN-1 silencing, Csi #2 (a) and Csi #3 (b) were less effective than Csi #1. Cytoplasmic localization of ZO-1 was observed in Csi #3-ZK-1 cells (f), but not in Csi #1-ZK-1 cells (e). For ZO-1 silencing, effect of Zsi #1 and Zsi #2 appeared to be similar as Zsi #3 in immunofluorescent staining (g, h), however, CLDN-1 translocation from cell membrane to cytoplasm was not obvious (c, d).

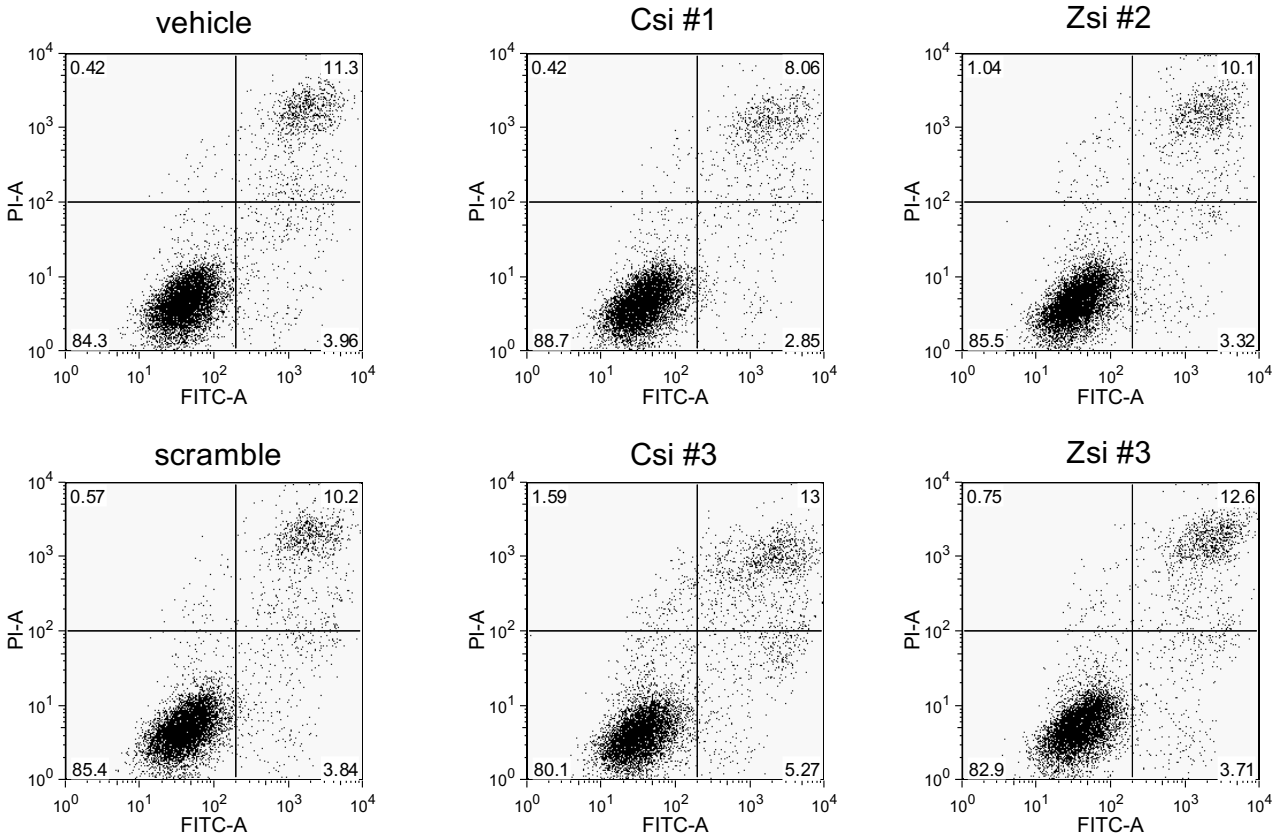


**Supplementary Figure 3.** Apoptosis assay in Csi/Zsi-transfected ZK-1 cells. Apoptosis assays did not detect a difference in death between the Csi/Zsi-transfected cells and the controls.